FORSCHUNGSZENTRUM
ROSSENDORF e.V.

FZR

FZR-70
Februar 1995
Preprint

M. Müller, F.-M. Dittes, W. Iskra and I. Rotter

Level repulsion in the complex plane

Forschungszentrum Rossendorf e.V.
Postfach 51 01 19 · D-01314 Dresden
Bundesrepublik Deutschland

Telefon (0351) 591 2091
Telefax (0351) 591 3700
E-Mail muellerm@fz-rossendorf.de

Level repulsion in the complex plane

M. Müller, F.-M. Dittes[1], W. Iskra[1,2] and I. Rotter[1,3]

[1] *Forschungszentrum Rossendorf, Institut für Kern- und Hadronenphysik, D-01314 Dresden, Germany*

[2] *Soltan Institute for Nuclear Studies, PL-00-681 Warszawa, Poland*

[3] *Technische Universität Dresden, Institut für Theoretische Physik, D-01062 Dresden, Germany*

Abstract

We consider the spectral properties of a model quantum system describing the coupling of bound states to a number of decay channels. We describe the separation of a few modes from the set of all resonances during the transition from low to high coupling strength between bound and continuum states (*trapping effect*) leading at high coupling to the formation of two time scales in terms of the life times of the resonance states. In particular, we give a detailed analysis of the critical region where the system finds its new resonance structure. Eigenvalues, eigenfunctions and their degree of mixing in relation to the corresponding wavefunctions of the closed system as well as cross sections are studied analytically and numerically for the cases of two and four resonances. For a multi-resonance case the dependence of these quantities on the spectrum of the underlying closed system is studied. We find that the global reorganization of the spectrum in the high coupling regime can be traced back to local redistributions acting on an energy scale comparable to the widths of the interfering resonances.

PACS: 03.65.Nk, 05.30.–d, 05.40.+j, 24.60.–k

1 Introduction

Recently, highly excited quantum systems have become of increasing interest in many areas of physics. Since at sufficiently high excitation energies many–particle systems have the possibility to decay, they should be treated as open ones [1]–[23]. As an immediate consequence, the quantum states have a finite lifetime.

In a microscopic theory of open many-particle quantum systems, the excited states of the system are constructed from the bound single-particle states (e.g. [7]). Nevertheless, they may have a finite lifetime if their energy is above the threshold for particle decay. The Hamiltonian of the many-body system is usually given in the form $H = H^0 + V$, where H^0 is a one-particle potential and V describes the residual interaction between the constituents. The latter one couples not only the unperturbed many-particle states (Slater determinants) one to each other leading to the discrete many-particle states, but also these discrete states to the open and closed decay channels. So in addition to the *internal coupling* between discrete states, also a coupling between bound and scattering states (*external coupling*) as well as a possible channel-channel coupling need to be considered. Due to this external coupling, the subspace of open decay channels forms an environment for the originally discrete states (*quasibound states embedded in the continuum* [7]). The system becomes open. The Hamiltonian of such an open quantum mechanical system is nonhermitian. Its eigenvalues are complex and determine both the energy positions and the inverse lifetimes (*widths*) of the states.

As it was shown in previous investigations (e.g. [21]), the transition from low to high values of the external coupling strength leads to a separation of a few resonances (*trapping effect*), which dominate the decay process. Initially, an increase of the external coupling strength causes a monotonic growth (in absolute value) of the imaginary parts of *all* complex eigenvalues of the effective Hamiltonian. This growth continues until the resonances start to overlap and the interference between neighbouring resonances becomes important. In a certain critical region, a *level repulsion in the complex plane* arises: A few eigenvalues gain a larger imaginary part while the other ones get a drift back to the real axis – in spite of the fact that the coupling to the open decay channels is increased –, i.e. they are getting trapped.

Thus, the structure of the system is, at low external coupling, comparable to that of the corresponding closed system. The corrections to the positions of the discrete states are small; the values of the partial widths can be calculated in the usual way by means of the spectroscopic and penetration factors. The structure of the resonance states at high coupling is, however, strongly influenced by the environment of decay channels: in the complex plane a hierarchy of states is formed which is strongly influenced by the structure of the environment, in particular by the number and the wavefunctions of the open decay channels.

It is the aim of this paper to investigate in detail the properties of an open quantum system in the critical region, where it finds its new order. In doing this, we incorporate the characteristics of an open system into a simple matrix model (chapter 2). The energies and total decay widths of the states of the system considered are calculated from the eigenvalues of a nonhermitian, effective Hamiltonian which can be constructed from the spectrum of the system of bound states together with their coupling vectors to the decay channels.

In a realistic calculation (e.g. in the framework of the nuclear shell model), the positions and wavefunctions of the discrete states are determined by the average potential and the residual interaction (internal mixing). In our calculation, we do not specify the internal coupling strength. We rather assume that it is contained implicitly in the spectrum of H^0, i.e. we simulate different internal mixings by studying different spectra of the Hamiltonian

H^0. The external mixing of the discrete states is given by an additional, complex–valued term in the effective Hamiltonian, which contains the coupling of the discrete states to the open decay channels. The channel-channel coupling is neglected in our calculations.

In section 3 and 4, we study the basic mechanism of the interaction of resonances by considering analytically and numerically the cases of two and four resonances. The level repulsion in the complex plane as well as other properties of the system are investigated at the critical point. In section 5, a more complicated case of 128 resonances and 8 open decay channels is treated numerically, in order to demonstrate how the local trapping of resonances influences successively the whole spectrum. Eigenvalues and eigenfunctions of the effective Hamiltonian are calculated for the multi-resonance case in dependence on the coupling strength to the decay channels. We examine the expansion coefficients of the wave-functions in relation to the eigenfunctions of the closed system and calculate the degree of mixing in relation to that basis. Using different spectra for the closed system, we investigate the role of the mean overlap of resonances for identifying the value of the critical coupling strength. Finally, as an example of an observable, the cross section of the two–resonance case is considered in section 6 as a function of the external coupling strength. Some conclusions from our results are drawn in the last sections.

2 The model

Our analysis is based on the following model (cf. Ref. [24]): We consider a quantum system consisting of $N > 1$ bound states $|\Phi_i^0\rangle, i = 1, 2, ..., N$, and K open two–body decay channels $|\chi_c(E)\rangle, c = 1, 2, ..., K$, which are coupled to the $|\Phi_i^0\rangle$ via a residual interaction $\hat{V}$. Supposed these states form an orthonormal set, the total Hamiltonian has the form

$$\mathcal{H} = \sum_{i,j=1}^{N} |\Phi_i^0\rangle H_{ij}^0 \langle\Phi_j^0| + \sum_{c=1}^{K} \int dE |\chi_c(E)\rangle E \langle\chi_c(E)| + \sum_{c=1}^{K}\sum_{i=1}^{N} \int dE \Big[|\Phi_i^0\rangle V_i^c(E) \langle\chi_c(E)| + h.c. \Big]. \tag{1}$$

Here, the H_{ij}^0 denote the matrix elements of the bound–state Hamiltonian. The vectors V^c with components $V_i^c(E) = \langle\Phi_i^0|\sqrt{\alpha}\hat{V}|\chi_c(E)\rangle$ are supposed to be pairwise orthogonal, which means a neglection of the direct reaction part. Their norm, or the average coupling matrix element $v_c^2 = \frac{1}{N}\sum_{i=1}^{N} |V_i^c|^2$, is a measure of the coupling strength to the corresponding channel c. By means of the coupling parameter α, we will vary the coupling strength between bound and scattering states. Additionaly, we restrict ourselves to time–reversal invariance. That allows us to choose all H_{ij}^0 and $V_i^c(E)$ real. Note that the *internal* coupling is given implicitly via the distribution of the eigenvalues of H^0.

If one neglects the potential scattering phase factor, the scattering matrix $S_{ab}(E)$ corresponding to the Hamiltonian $\mathcal{H}$ can be written in the form [24]

$$S_{ab}(E) = \delta_{ab} - 2\pi i \sum_{i,j} V_i^a(E) \Big[\Big(E - H^{eff}(E) \Big)^{-1} \Big]_{ij} V_j^b(E) \,, \tag{2}$$

where b and a denote the in- and outgoing channel, correspondingly, and

$$H^{eff}(E) = H^0 + F(E) \tag{3}$$

is the effective Hamiltonian in the subspace of bound states. Due to the second term $F(E)$, H^{eff} contains explicitely the coupling to the environment of decay channels. The matrix

elements of the operator $F(E)$ are

$$F_{ij}(E) = \sum_c \int dE' \frac{V_i^c(E')V_j^c(E')}{E^{(+)} - E'}. \tag{4}$$

We restrict ourselves to an energy region far away from decay thresholds. Then the vectors V^c can be considered as energy independent. In this case F_{ij} is purely imaginary and energy–independent, as well:

$$F_{ij} = -i\pi \sum_{c=1}^{K} V_i^c V_j^c \,, \tag{5}$$

so that H^{eff} takes the form

$$H^{eff} = H^0 - i\pi \cdot VV^+. \tag{6}$$

In our analysis, we consider the complex eigenvalues of the effective Hamiltonian as a function of the coupling strength parameter α. Furthermore, we analyse the behavior of the corresponding eigenfunctions, $|\Phi_R\rangle$, and their mixing via the decay channels for each resonance in dependence on α.

First, let us consider the eigenfunctions. Due to the nonhermiticity of the effective Hamiltonian H^{eff} one has to distinguish between its left and right eigenvectors:

$$H^{eff}|\Phi_R^r\rangle = \mathcal{E}_R|\Phi_R^r\rangle \tag{7}$$

$$(H^{eff})^+|\Phi_R^l\rangle = \mathcal{E}_R^*|\Phi_R^l\rangle \tag{8}$$

with

$$\mathcal{E}_R = E_R - \frac{i}{2}\Gamma_R \,. \tag{9}$$

Since H^{eff} is symmetric, it can be diagonalized by a complex orthogonal matrix B fulfilling

$$BB^T = B^T B = 1 \,. \tag{10}$$

The (complex) matrix elements $b_{RR'}$ of B connect the eigenvectors $|\Phi_R^r\rangle$ and $|\Phi_R^l\rangle$ to the eigenvectors $|\Phi_R^0\rangle$ of the bound state hamiltonian H^0:

$$\begin{aligned} |\Phi_R^r\rangle &= \sum_{R'} b_{RR'}|\Phi_{R'}^0\rangle \\ |\Phi_R^l\rangle &= \sum_{R'} b_{RR'}^*|\Phi_{R'}^0\rangle \end{aligned} \tag{11}$$

and, correspondingly,

$$\begin{aligned} \langle\Phi_R^r| &= \sum_{R'} b_{RR'}^*\langle\Phi_{R'}^0| \\ \langle\Phi_R^l| &= \sum_{R'} b_{RR'}\langle\Phi_{R'}^0| \,. \end{aligned} \tag{12}$$

Eq. (10) implies the bi-orthogonality relation

$$\langle\Phi_R^l|\Phi_{R'}^r\rangle = \delta_{RR'} \,. \tag{13}$$

On the contrary, the right eigenvectors as well as the left ones are, in general, not orthonormal among themselves:

$$\langle \Phi_R^\tau | \Phi_{R'}^\tau \rangle \neq \delta_{RR'} \,. \tag{14}$$

In the following, we will use the right eigenvectors only, and denote $|\Phi_R^\tau\rangle$ simply by $|\Phi_R\rangle$.

After considering the eigenvalues of H^{eff} the next quantity of our interest is the α–dependence of the scalar product $\mathcal{N}_R \equiv \langle \Phi_R | \Phi_R \rangle$. As mentioned above, due to the non-hermiticity of H^{eff} it is not normalized to one, and its deviation from unity may serve, therefore, as a measure of the 'degree of openess' of the system. From eqs. (11) and (12) we get

$$\mathcal{N}_R \equiv \langle \Phi_R | \Phi_R \rangle = \sum_{R'} b^*_{RR'} b_{RR'} = \sum_{R'} |b_{RR'}|^2 \tag{15}$$

which is real and ≥ 1 since

$$\begin{aligned} \sum_{R'} |b_{RR'}|^2 &= \sum_{R'} ((\Re b_{RR'})^2 + (\Im b_{RR'})^2) \\ &\geq \sum_{R'} ((\Re b_{RR'})^2 - (\Im b_{RR'})^2) = \Re \sum_{R'} (b_{RR'})^2 = (BB^T)_{RR} = 1 \,. \end{aligned} \tag{16}$$

For very small α we have a nearly closed system and, therefore, $\mathcal{N}_R(\alpha) \approx 1$. With increasing α the values of $\mathcal{N}_R(\alpha)$ are expected to grow on in dependence on the mixing of the different original states. A detailed discussion of the behaviour of $\mathcal{N}_R(\alpha)$ will be given in the next two sections.

Another quantity reflecting the mixing of a given state R relative to the eigenstates of the bound state Hamiltonian H^0 caused by the second term, $F(E)$, in H^{eff} is the *external mixing*

$$I_R = -\sum_{R'} |\hat{b}_{RR'}|^2 \ln |\hat{b}_{RR'}|^2 \,. \tag{17}$$

Such a definition is motivated by the relation of the external mixing to the information entropy I given by $I = \sum_R I_R$ [17]. The coefficients $\hat{b}_{RR'}$ in eq. (17) are obtained from the $b_{RR'}$ (cf. eqs. (11) and (12)) by a simple rescaling, so as to obey the requirements for probability amplitudes:

$$0 \leq |\hat{b}_{RR'}|^2 \equiv \frac{|b_{RR'}|^2}{\sum_{R'} |b_{RR'}|^2} \leq 1 \,. \tag{18}$$

3 The basic mechanism of trapping

Let us first investigate the simple case of two resonances and one open decay channel.

A theoretical study of interference effects in two–resonance systems can be found in [2, 14]. An experimentally accessible example of such a system is the isospin doublet of 2^+-resonances in ^8Be [6, 14]. These resonances have approximately the structure of $^7Li + p$ and $^7Be + n$, and they are lying at excitation energies around 16.6 and 16.9 MeV. A detailed experimental investigation of these resonances in ^8Be was performed in [25]. As a consequence of the isospin symmetry of the nuclear force on one hand, and of the symmetry of the two configurations with respect to the Coulomb force on the other hand, this doublet is expected to be nearly degenerate. This means that the two resonances are in strong interference one

with each other and are obviously close to the critical point of trapping.

The simple example of two states and one open decay channel allows to investigate the basic process of the repulsion of two complex eigenvalues most clearly. The coupling vector V (normalized to length $\sqrt{\frac{2\alpha}{\pi}}$) is determined by a single angle φ: $V = \sqrt{\frac{2\alpha}{\pi}}(\cos\varphi, \sin\varphi)$, so that eq. (6) can be written as

$$H^{eff} = \begin{pmatrix} 1 & 0 \\ 0 & -1 \end{pmatrix} - 2i\alpha \begin{pmatrix} \cos^2\varphi & \cos\varphi\sin\varphi \\ \cos\varphi\sin\varphi & \sin^2\varphi \end{pmatrix}, \tag{19}$$

where without loss of generality we have chosen the eigenvalues of H^0 to be ± 1. In this case of two resonances and one open decay channel, the symmetry of the problem is completely determined by the coupling vector. By means of the angle φ either one of the resonances couples stronger to the decay channel than the other one or both couple with the same strength ($\varphi = \frac{\pi}{4}$). The eigenvalues of this matrix are:

$$\mathcal{E}_\pm = -i\alpha \pm \sqrt{1 - 2i\alpha \cdot \cos 2\varphi - \alpha^2}. \tag{20}$$

The influence of the parameter φ in the Hamiltonian (19) onto the eigenvalue picture is illustrated by means of Figs. 1.a and 1.b. The motion of the eigenvalues is drawn here as a function of the coupling strength α for two different values of φ (Note that for $\varphi = \pi/4$ the totally symmetrical situation is generated, where both resonances couple with equal strength to the decay channel). In both cases an attraction of the levels in the complex plane is observed for values $\alpha < \alpha_{crit}$ and a repulsion for $\alpha > \alpha_{crit}$. Here, α_{crit} is defined as that value of α, at which the two resonances are in a minimal distance one from each other. That means, α_{crit} is a local parameter defined as the critical point at which the level attraction of two resonances turns into level repulsion. Note that the attraction of the resonances for $\alpha < \alpha_{crit}$ corresponds to an attraction of the real parts of the eigenvalues (i.e. of their positions in energy) only. Analogously, the level repulsion for $\alpha > \alpha_{crit}$ affects only the imaginary part; in particular, for $\varphi = \frac{\pi}{4}$ the two states are found to be degenerate in energy.

For a given bound state spectrum, the minimal distance of the two eigenvalues in the complex plane is determined by the symmetry of the coupling vector V. In the case of eq. (19) with total symmetry of V ($\varphi = \frac{\pi}{4}$) the minimal distance is zero, while it is larger than zero for other φ (compare Figs. 1.a and 1.b).

It is interesting to trace also the quantity $\mathcal{N}_R(\alpha)$, eq. (15), for each resonance. A simple analytical expression for $\mathcal{N}_R(\alpha)$ can be obtained for the case of a symmetrical vector V. Let us denote the eigenfunctions of H^{eff} normalized according to eq. (13) by

$$|\Phi_\pm\rangle = N_\pm \cdot \begin{pmatrix} 1 \\ \phi_\pm \end{pmatrix} \tag{21}$$

with $N_\pm = 1/\sqrt{1+\phi_\pm^2}$. From eqs. (7) and (20) one easily finds that $\phi_\pm = \frac{1}{\alpha}\cdot(\pm\sqrt{\alpha^2-1} - i)$. The critical value of the coupling strength α is determined by the requirement $\mathcal{E}_+ = \mathcal{E}_-$ (cf. eq. (20) for $\varphi = \frac{\pi}{4}$) giving $\alpha_{crit} = 1$. Because of the total symmetry of the coupling matrix, the two states are degenerate in real energy for $\alpha \geq 1$. In the three interesting limits $\alpha \to 0, \alpha \to 1$ und $\alpha \to \infty$ the wavefunctions $|\Phi_\pm\rangle$ are:

$$\begin{aligned}
&\alpha = 0: \quad \phi_\pm = \begin{cases} 0 \\ \infty \end{cases} \quad \Rightarrow \quad \Phi_+ = \tbinom{1}{0}, \qquad \Phi_- = \tbinom{0}{1} \\
&\alpha \to \infty: \quad \phi_\pm \to \pm 1 \quad \Rightarrow \quad \Phi_+ \to \tfrac{1}{\sqrt{2}}\tbinom{1}{1} \qquad \Phi_- \to \tfrac{1}{\sqrt{2}}\tbinom{1}{-1} \\
&\alpha \to 1: \quad \phi_\pm \to -i \quad \Rightarrow \qquad\qquad \Phi_+ = \Phi_- \to \tbinom{0}{-i}\cdot\infty
\end{aligned} \tag{22}$$

From the last equation one sees that at $\alpha = \alpha_{crit} = 1$, where the two eigenvalues coincide in the complex plane, the scalar product of the wavefunctions goes to infinity:

$$\mathcal{N}_{\pm}(\alpha)\Big|_{\alpha\to 1} \longrightarrow \infty \,. \tag{23}$$

For $\varphi \neq \pi/4$ the singularity of $\mathcal{N}_{\pm}(\alpha)$ at $\alpha = \alpha_{crit}$ is replaced by a finite maximum.

Let us now consider the information entropy. For the case of the two resonances and one open decay channel, eqs. (17), (18) and (21) give the result ($R = \pm$; $R' = 1, 2$; $b_{\pm 1} = N_{\pm}$; $b_{\pm 2} = N_{\pm}\phi_{\pm}$)

$$\begin{aligned} I_{\pm}(\alpha) &= \ln 2 - \frac{\alpha^2}{1-\sqrt{1-\alpha^2}} \ln \alpha \\ &\quad + \left[\frac{\alpha^2}{1-\sqrt{1-\alpha^2}} - 1\right] \cdot \ln\left(1-\sqrt{1-\alpha^2}\right), \end{aligned} \tag{24}$$

for the range $0 < \alpha \leq 1$, whereas for $\alpha \geq 1$ the external mixing function is given by

$$I_{\pm}(\alpha) = \ln 2. \tag{25}$$

From eqs. (24) and (25) we see that the two mixing coefficients $I_{\pm}$ are equal to each other. It can be proven that this result is true not only in the case of symmetrical coupling considered here, but remains valid for any coupling of two resonances to one channel, i.e. for arbitrary φ. Indeed, taking into account the relations (11) and (12), the bi-orthogonality condition (13) implies that

$$(\Phi_{\pm}^{(1)})^2 + (\Phi_{\pm}^{(2)})^2 = 1 \tag{26}$$

and

$$\Phi_{+}^{(1)}\Phi_{-}^{(1)} + \Phi_{+}^{(2)}\Phi_{-}^{(2)} = 0 \,. \tag{27}$$

Taking the square of the last equation and inserting the resulting expression into eq. (26), we find

$$(\Phi_{\pm}^{(2)})^2 = (\Phi_{\mp}^{(1)})^2 \,, \tag{28}$$

and, consequently,

$$|\Phi_{\pm}^{(2)}|^2 = |\Phi_{\mp}^{(1)}|^2 \,. \tag{29}$$

From eq. (29), one immediately sees that in the case of two resonances and one decay channel it always holds $\mathcal{N}_{+}(\alpha) = \mathcal{N}_{-}(\alpha)$ and $I_{+}(\alpha) = I_{-}(\alpha)$.

As a result of the investigation of the two–resonance one–channel case we state the following:

(i) By switching on the coupling to the environment, the states of the underlying closed system become unbound. The energy positions and lifetimes of the two resonance states follow from the eigenvalues of an effective non-hermitian Hamiltonian. The movement of the eigenvalues in the complex plane as a function of the coupling parameter α shows an increase of the imaginary parts of the two eigenvalues, and an attraction of their real parts as long as the coupling is below α_{crit}. At $\alpha = \alpha_{crit}$, the eigenvalues have a minimal distance in the complex plane, which depends on the symmetry of the continuum coupling and the internal mixing of the bound states. The value α_{crit} is therefore a locally defined quantity, describing a critical point of *two* interfering resonances. At larger values of α, a repulsion of the imaginary parts is observed.

(*ii*) The process of rearrangement is also reflected in the eigenfunctions. Because of the nonhermiticity of H^{eff}, $\langle\Phi_\pm|\Phi_\pm\rangle$ is not normalized to unity. For very small as well as for high values of the coupling strength we have $\langle\Phi_\pm|\Phi_\pm\rangle \approx 1$ like in a closed system, which is described by a hermitian Hamiltonian. But for values of α near to the critical point, $\langle\Phi_\pm|\Phi_\pm\rangle$ differs strongly from 1. The maximum value of $\langle\Phi_\pm|\Phi_\pm\rangle$ is reached at the critical point where the eigenvalues have the minimal distance from each other. The more the two resonances touch each other, that means the smaller the minimal distance is, the larger is the value for $\langle\Phi_\pm|\Phi_\pm\rangle$. In the totally symmetrical case of two resonances it goes to infinity.

(*iii*) Further, the mixing of the wavefunctions, $I_\pm(\alpha)$, is rising with the external coupling strength α up to the point where $\alpha = \alpha_{crit}$. In the symmetrical two–resonance case the external mixing reaches its maximal possible value of $\ln 2$ and stays constant for $\alpha > \alpha_{crit}$.

4 The four–resonance, one–channel case

Before investigating the general case of many resonances and more than one decay channel, we present results obtained for four resonances coupled to one decay channel. This case is still a simple one. It is, however, free of the peculiarites of the two–resonance case and contains already the whole variety of phenomena characteristic for the many–resonance case. We traced the eigenvalue picture of H^{eff} as well as the function I defined by eq. (17) for both a symmetrical and an asymmetrical distribution of the bound states and for the two coupling vectors $V_1 = 1/2\{1,1,1,1\}$ and $V_2 = 1/2\{1,-1,1,-1\}$.

In Fig. 2 the results are presented for a bound state spectrum symmetrical around 0 ($E_1 = -1, E_2 = -1/3, E_3 = 1/3, E_4 = 1$) and the completely symmetric coupling vector V_1. Fig. 2.a shows that, although all bound states couple with the same amplitude to the decay channel, the drift velocity of the four eigenvalues is different. The two resonances lying at the border of the spectrum get trapped first by the two inner states. Since the neighborhood of the two two–resonance systems ($|1> \,\&|2>$ and $|3> \,\&|4>$) is not symmetric, these trappings resemble the situation of Fig. 1.b. The two local broad modes formed interfere at further increasing values of α in a symmetrical way, leading to the middle part of Fig. 2.a.

In Fig. 2.b the mixing functions I_R for the four resonances are displayed. One sees that the functions I_2, I_3 increase stronger than the I_1, I_4. This is due to the fact that the two states in the middle of the spectrum interfere in a constructive way already for small α with left *and* right neighbors. As a result, they have both a larger mixing (cf. Fig. 2.b) and a larger *effective* coupling to the decay channel – resulting in a larger width (cf. Fig. 2.a). Note, that with increasing α any eigenstate of H^{eff} differs more and more from the original bound state at $\alpha = 0$ by collecting admixtures from *all* eigenstates of H^0. The relative signs of these admixtures determine the specific interferences and lead to the behaviour shown in Fig. 2. The behaviour of I_R for larger α, approaching a constant for the states $|1>$ and $|4>$ and having even a decreasing tendency for the resulting antisymmetric combination of states $|2>$ and $|3>$ is due to the negative interference between different admixtures. Since the wave functions of the two states which are trapped at the first stage of the process do not change significantly with a further increase of α, their mixing functions remain almost constant, whereas the antisymmetrization during the resonance repulsion at the second hierarchy level (between resonances $|2>$ and $|3>$) leads effectively even to a decrease of the corresponding mixing function.

Fig. 3 contains the analogous data for the asymmetric bound state spectrum $E_1 = -1, E_2 = -0.8, E_3 = 1/3, E_4 = 1$. Here the results are similar to those discussed above. The

main differences, caused by the distortion of symmetry, consist in the absence of a point of total degeneracy of two eigenvalues in the complex plane, and in the resulting mixing functions.

In all cases shown in Figs. 2 and 3, the maximal value $I_R = \ln 4$ is reached only for the short–lived state. This is in contrast to the two–resonance, 1–channel case discussed in section 3 where we found $I_R = \ln 2$ (for $\alpha > 1$) for both the short–lived and the long–lived resonance. This is connected to the fact that the external mixing is produced at the critical points. As a consequence, the number of critical points passed by a resonance during its evolution determines its mixing, and broad modes gain, with increasing α, a larger value of I_R as compared to the majority of trapped states.

Another quantity reflecting the rotation of the states under the influence of the external coupling, $1/N|\sum_{R'} b_{RR'}|$, is traced in Fig. 4. At small coupling strength all eigenvectors are normalized and orthogonal one to each other, and the corresponding functions start at 0.25. Reflecting the increasing interference, with rising α the eigenvectors are rotating in Hilbert space towards each other. This corresponds to the attraction of eigenvalues observed for those α. At the critical point the eigenvalues reach their minimal distances, and the mixing coefficients $b_{RR'}$ change most rapidly. Finally, at high coupling the eigenvectors are getting more and more orthogonal again. The broad mode which is formed in the strong coupling region, points (in Hilbert space) asymptotically exactly into the direction of the coupling vector and the corresponding value of $1/N|\sum_{R'} b_{RR'}|$ is sensitive, therefore, to the relative signs in the two coupling vectors introduced above. The interference between different resonances decreases again although the broad mode covers all of the trapped states, and we arrive at a situation of overlapping but almost not interfering resonances.

Summarizing, we state that an investigation of the basic process of trapping allows us to understand the reorganization occuring in many-particle quantum systems at high level density. The basic process can be investigated numerically and analytically without further approximations.

5 The many–resonance, many–channel case

We turn now to more complex situations. As an example we present the results obtained for 8 open decay channels ($\mathrm{rank}[F_{ij}] = 8$) and 128 bound states given by the eigenvalues of the matrix H^0. Two different initial distributions of the bound states are considered: In the first case a uniform distance between the states is chosen, so that the states are lying symmetrically around some value chosen arbitrarily at $E_0 = 0$ (cf. Fig. 5.a). In the second case 100 bound states are placed in the same manner, symmetrically around the E_0, but with a much smaller distance. The remaining 28 bound states are placed with a larger next–neighbour distance, but also uniformly around the energy region of the dense lying states with a slightly shifted center (Fig. 6.a). Thus, the 128 states are distributed over a certain energy interval in a different manner in the both cases.

We performed the investigations as a function of the external coupling to the open decay channels. As we will show below, the behaviour of the system can be described as a successive pairwise action of eigenvalue collisions in the complex plane, as described in section 2. Generated by this basic process, a hierarchical arrangement of complex eigenvalues with respect to their imaginary parts is generated.

Fig. 5.a shows the motion of the eigenvalues $E_R + \frac{i}{2}\Gamma_R$ of the effective Hamiltonian H^{eff} in the complex plane as a function of α for the case of the uniform initial distribution of the

bound states. Like in the two–resonance case, all of the eigenvalues move into the complex plane with increasing α – up to a critical value of α at which trapping arises. Note that this value is an individual one for every pair of resonances. It depends on the positions of the resonances in the spectrum and on their coupling amplitudes to the decay channels.

At still larger values of α some of the resonances are getting long-lived as a consequence of trapping, while the widths of the remaining ones increase more rapidly than before. The broad resonances envelop the underlying narrow resonances which do no longer disturb the propagation of the broad resonances. With a further increase of α, the broad states get into conflict with other broad resonances in their *new* neighbourhood of eigenvalues. Again, each pair of interfering resonances reaches a certain critical point of α, where trapping occurs. So, with increasing α, successively more and more resonances are getting trapped. This goes further up to that point, where only K broad states remain ($K = 8$ is equal to the number of open decay channels $\equiv \mathrm{rank}[F_{ij}]$). They are no longer coming into conflict one with each other by a further increase of α (note that channel–channel coupling is not contained in our calculations).

The individual critical points for the different eigenvalue collisions are clearly visible in Fig. 5.b where the imaginary part of the complex eigenvalues of H^{eff} is displayed as a function of the coupling parameter α. Caused by the special symmetrical distribution of the discrete eigenvalues of H^0, two resonances follow always one curve in figure 5.b.

Coming back to the discussion in section 3, Figs. 5.a and 5.b display both, the symmetrical and nonsymmetrical collisions of two eigenvalues. Only in that case, when the two colliding resonances have exactly the same widths (which means that they are lying symmetrically relative one to each other and have equal coupling to the decay channels) the minimal distance equals 0. In this case with full symmetry, the energy attraction for $\alpha \leq \alpha_{crit}$ and width repulsion for $\alpha > \alpha_{crit}$ can be seen most clearly. The two resonances stay degenerate in energy above the critical coupling strength α_{crit}. The overlapping of both resonances is not avoided.

The symmetry of the resonance distribution is determined by the two parts of the effective Hamiltonian, H^0 and F. In our model, H^0 is chosen with vanishing non-diagonal matrix elements, while the diagonal matrix elements are set by hands. The nonhermitian part F contains the coupling to the environment of decay channels. Both parts determine the symmetry of the problem and therefore the minimal distances in the eigenvalue collisions, as shown in Fig. 1. As a result, successive energy attraction and width repulsion is produced, at some critical values of α, which is based on a local mechanism, acting on an energy scale of the order of magnitude of the widths of two interfering resonances. The result is a global figure of hierarchically (with respect to their widths) arranged eigenvalues of the whole spectrum.

Not only the complex eigenvalues of the effective Hamiltonian show signatures of this reorganisation process, but also the eigenfunctions. As shown in Fig. 5.c, the scalar product $\mathcal{N}_R = \langle \Phi_R | \Phi_R \rangle$ is sensitive to the redistribution of the resonant states. The values of $\mathcal{N}_R$ for the 8 broadest states are drawn in thick points. One sees that for very small α (i.e. in the regime of well separated resonances), the values of all $\mathcal{N}_R$ are close to one. Whenever $\alpha \approx \alpha_{crit}$, level repulsion of two resonances occurs and a maximum value of the corresponding $\mathcal{N}_R$ is reached. For $\alpha > \alpha_{crit}$, they are going back to values close to one. The sharpness of the peak and the maximum of its value are a measure of how close the eigenvalues of the two repelling resonances, which got into conflict, are coming to each other. Thus, the symmetry of the problem is reflected also in the wavefunctions. That means, the smaller the minimal distance of two eigenvalues in the complex plane, the larger are the values of the

$\mathcal{N}_R = \langle \Phi_R | \Phi_R \rangle$. If the resonance overlapping at the critical point of α is not avoided (total symmetry of two interfering resonances), a degeneracy is produced and the corresponding $\mathcal{N}_R$ rise to infinity at $\alpha = \alpha_{crit}$.

Fig. 5.d shows the mixing coefficients I_R of the eigenfunctions of H^{eff} relative to the basis of bound states (eigenfunctions of H^0) as a function of α. The critical points are clearly visible also in this function: The I_R increase strongly up to the point where the level repulsion takes place. At these points the wavefunctions suffer crucial changes (Fig. 5.c). Beyond the critical region ($\alpha > 5.8 \cdot 10^{-3}$), the mixing coefficients of both, the broad and the trapped wavefunctions saturate at a constant value which is, however, lower than the equilibrium value $I_{equi} = \ln 128 = 4.852$.

In Fig. 6.a-d the results obtained for the second (non-uniform) initial distribution are displayed. The qualitative characteristics of the Figures 5 and 6 are the same. In both cases the hierarchical rearrangement of the eigenvalues caused by the local mechanism of trapping of resonances, which takes place successively with increassing α is observed. It is remarkable, that – contrary to the case with uniform distribution shown in Fig. 5 – all the broad states arise from the region of high level density. The chance of a strong interference and therefore of an eigenvalue collision is much higher in this energy interval than in the other one with lower level density. As a consequence, more critical points appear up to a certain α, and the widths of the broad states are larger than those of the states in the low-density region. As a result, the 8 broad states of the highest hierarchy are already formed, when the 28 remaining resonances of the region of low level density start to take part in the interference process. Therefore, they have the only chance to get trapped.

Summarizing the results obtained up to now, we conclude that the global picture for the eigenvalue distribution of the effective Hamiltonian is created by an effect which acts in local energy regions. This behaviour is independent of the chosen initial distribution. With growing coupling to the environment a sequence of critical points arises in any case, i.e. attractions and repulsions of eigenvalues in the complex plane occur. This process terminates when the number of broad modes is equal to the rank of the coupling matrix, which is equal to the number of open decay channels. These broad resonances survive independently one from each other and no further level repulsion will occur. Therefore, it is naturally to define the critical point α_{crit}^{sys} of the system as that value of α, at which K states are separated from the rest of the resonance states.

With this definition, α_{crit}^{sys} turns out to be different for the two considered initial distributions chosen by us. Averaged over the whole spectrum, however, both systems start with the same value of the mean level distance $\bar{D}$.

Fig. 7 displays the ratio of the mean resonance width to the mean level distance, $\bar{\Gamma}/\bar{D}$, for the uniform initial distribution (dashed curve), for the distribution of a region of high and low level density (solid line) and separately for the region of high level density alone (dotted curve) as a function of α. The critical points for the three situations are indicated. As can be seen, a nearly linear relation between $\bar{\Gamma}/\bar{D}$ and α exists. Besides of this, the first two curves show approximately the same slope. As a consequence, not only α_{crit}^{sys} is different for the cases considered, but also the corresponding value of $(\bar{\Gamma}/\bar{D})_{crit}^{sys}$.

The critical values $(\bar{\Gamma}/\bar{D})_{crit}^{sys}$ for the first two cases considered above differ by a factor of ≈ 3. If one considers only the region of high level density (third case), where the main process of the rearrangement of the system occurs, the difference is even larger.

We conclude that the critical point of the system can not be determined from the knowledge of only $\bar{\Gamma}/\bar{D}$. The probability of eigenvalue collisions is surely connected with $\bar{\Gamma}/\bar{D}$, and the chance that the value of α_{crit}^{sys} is reached and the last hierarchy is formed is higher for larger values of $\bar{\Gamma}/\bar{D}$. But no definite conclusions concernig the critical point can be drawn for any fixed number of $\bar{\Gamma}/\bar{D}$. The critical point does not scale by means of that quantity. As can be seen in the second example, $\bar{\Gamma}/\bar{D}$ depends also on the energy region taken into account. If one considers only the region of high level density, the critical value of $\bar{\Gamma}/\bar{D}$ is much larger than in the other case. In that region, most of the eigenvalue collisions occur and all of the broad modes arise from it. The remaining 28 resonances at the border are getting trapped, when the global process of trapping has already terminated and the 8 broad states have been formed. These facts call for caution in using $\bar{\Gamma}/\bar{D}$ for the classification of a system with respect to the trapping effect. They emphasize the importance of the local, individual processes for the global redistribution of resonances.

Based on these results, we point out that a hierarchical formation of the eigenvalues occurs due to local fluctuations of the level density. The global rearrangement is generated by the local mechanism of attraction and repulsion of two eigenvalues in the complex plane. Features of this process can be seen also in the corresponding wavefunctions: The values $\mathcal{N}_R(\alpha)$ and $I_R(\alpha)$, defined in section 2, reflect the evolution of the system in a significant manner. Finally, we saw that regions of high level density are regions favoured for trapping. One has to keep in mind, however, that $\bar{\Gamma}/\bar{D}$ does not determine quantitatively neither the local level collisions nor the global value α_{crit}^{sys}. It is impossible to decide, for any fixed value of $\bar{\Gamma}/\bar{D}$, at which stage the reorganisation process in the system actually is.

6 The cross-section

In order to investigate in which manner the trapping effect can be seen in an observable quantity, we have calculated the cross section of the symmetrical two–level system described analytically in section 3. The cross section is calculated from $|1-S|^2$ with the expression for the S-Matrix given by eq. (2). We considered a symmetrical situation of two states coupled with equal strength to one open decay channel.

The three–dimensional Figure 8 shows the total cross section over the interesting energy range as a function of α. In Fig. 9.a-c the total cross section for three values of α ($\alpha = 0.08,\ 1,\ 4$) is displayed separately (solid lines). In order to demonstrate the importance of interference effects, two Breit-Wigner curves are drawn (dashed lines) – with parameters corresponding to the energies and widths given by the complex eigenvalues of the effective Hamiltonian. So the dashed lines give the picture of the cross section if one assumes isolated states which do not interfere one with each other.

For small α the resonances are well isolated, they have small widths and their overlap is nearly zero. The cross section in the small coupling regime is well approximated by the two Breit–Wigner curves. Then, with increasing α, one observes a strong increase of the average cross section up to the maximum value 4, and the resonance structure is getting broader. Besides of the increasing widths of the resonances, there is an energy shift in the position of each eigenvalue in the direction to the other one. Therefore, a strong overlap is produced. At $\alpha = 1$, the critical point of level repulsion is reached. At this point both eigenvalues are placed at the same point in the complex plane (see also figure 1.a). Both resonances have the same lifetime and the same energy position.

With a further increase of α one of the resonances gets trapped, while the other eigen-

value receives a strong drift into the complex plane (cf. Fig. 1.a). The latter eigenvalue dominates the decay behaviour of the system. There is no energy shift in the range $\alpha > \alpha_{crit}$, i.e. at high coupling strength the energy positions of both resonances stay constant.

The cross section is changing from the figure of two well separated resonances with nearly a Breit–Wigner shape to a situation where only a dip in a broad structure can be seen. At $\alpha \geq \alpha_{crit}$ the minimum in the cross section at $E = 0$ is caused purely by interference – what can be seen best in the cross section picture at $\alpha = 1$.

Generally, it is difficult to draw conclusions on the positions and widths as well as on the strength of the two resonances if one knows only the cross section. At $\alpha = 1$, the cross section seems to be caused by the existence of two resonances lying at the energies which the states at $\alpha = 0$ had. That means, the level attraction for small α cannot be seen in the cross section. Further, the area of the two resonances is smaller than the area of the two (isolated) Breit-Wigner resonances. Thus, the analysis of the total cross section would lead not only to incorrect conclusions concerning the positions of the resonances but also to widths and transition strenghts being too small. In this case, the *missing strength* is a result of the interferences (see also [26] for a realistic situation).

As a consequence, one can follow the reorganisation process only from the explicit knowledge of the eigenvalues or eigenfunctions, i.e. it is necessary to measure directly the different time scales. In nuclear physics, the existence of different time scales is very well known for a long time and described by phenomenological models such as the doorway concept. A direct measurement of the different time scales became possible recently in molecules [27]. The results obtained there support the conclusions drawn in the present work.

We would like to emphasize the smooth behaviour of σ *at* the critical value, $\alpha_{cr} = 1$. Indeed, as discussed in section 3, for $\alpha = 1$ the S-matrix has a double pole, and quantities like the scalar product $\mathcal{N}$ diverge. Nevertheless, one can prove that observable quantities deduced from the S-matrix at the real energy axis are well defined. In particular, the unitarity of the S-matrix is not affected by this double pole.

In order to check this statement, we note that in the case of two states and one open channel the formula (2) for the S-matrix reads

$$S(E,\alpha) = 1 - 2\pi i \cdot \sum_{\pm} \frac{\tilde{V}_{\pm}^2}{E - \mathcal{E}_{\pm}}, \tag{30}$$

where the $\tilde{V}_{\pm}$ are the transition matrix elements $\langle \Phi_{\pm} | \sqrt{\alpha} \hat{V} | \chi \rangle$ between the bound states $|\Phi_{\pm}\rangle$ and the channel wavefunction $|\chi\rangle$. Introducing the partial width $\gamma_{\pm} = \frac{1}{2\pi} |\langle \Phi_{\pm} | \sqrt{\alpha} \hat{V} | \chi \rangle|^2$ and using the relation $\gamma_{\pm} = \langle \Phi_{\pm} | \Phi_{\pm} \rangle \Gamma_{\pm}$ between partial and total widths [28], the S-matrix reads

$$S(E,\alpha) = 1 - i \cdot \sum_{\pm} \frac{\langle \Phi_{\pm} | \Phi_{\pm} \rangle \Gamma_{\pm}}{E - \mathcal{E}_{\pm}} \,. \tag{31}$$

As derived in section 2, $\langle \Phi_{\pm} | \Phi_{\pm} \rangle \equiv \mathcal{N}_{\pm}$ diverges at $\alpha = \alpha_{crit}$. Nevertheless, inserting eqs. (20) and (21) into the obtained expression for $S(E,\alpha)$, we see that

$$S(E,\alpha) = \frac{1 - E^2 + 2iE\alpha}{1 - E^2 - 2iE\alpha} \tag{32}$$

which is unitary for real E and for any α. Note that the same result can be obtained without introducing the notion of partial width by taking into account that $\tilde{V}_{\pm} = \sum_{l=1}^{2} V^{(l)} \Phi_{\pm}^{(l)}$ with

$V^{(1)} = V^{(2)} = \sqrt{\alpha/\pi}$.

Concluding this section, we see that the trapping effect is hidden in the total cross section in a complicated manner. Even in the simple two–resonance case, it is difficult to resolve the two time scales created at high level density. Much more complicated is the interference picture in the many–resonance case. In the many–resonance one–channel case, only sharp dips embedded in a background of very broad resonances arise. There is, however, some evidence the short and long-lived resonances show a different angular dependence in the *differential* cross sections which we will discuss in a subsequent paper. Nevertheless, reliable conclusions on the trapping of resonances can be drawn only from direct lifetime measurements.

7 Conclusions

In open systems two types of forces appear. The structure of the underlying closed system is given by internal forces while a so-called external force couples the system to the environment and regulates the energy- or particle flow to it. Due to this coupling new features are generated in the system: properties from the environment are imprinted onto the internal structure. So the internal force stabilizes the properties of the underlying closed system, whereas the external one induces new properties under the influence of the environment. If one examines the evolution of the system with growing external force, one observes a critical region, where the system reorganizes itself. Structural properties from the environment are now visible, and in a comparable small interval of the external coupling the system finds a new structure.

The variation of the external coupling strength allows an examination of the properties of the open system in relation to those of the corresponding closed one. The transition from the situation of equal distribution of the lifetimes to the hierarchical formation of the eigenvalues in the complex plane is traced by us as a function of the external coupling strength. As we have shown, this transition arises successively. It is determined by the local properties of the level density for the discrete states as well as by the specific form of the coupling vectors between bound states and continua. Critical points in the coupling strength arise, when the resonances interact with resonances from their neighbourhood, i.e. with resonances neighbouring in energy, and having lifetimes of the same order of magnitude. Successively, with increasing external coupling one critical point after the other is reached. The local effect of trapping of neighbouring resonances produces a global picture of a hierarchical formation of the eigenvalues of all resonances in the complex plane. The resonances of different hierarchies are not interfering with each other due to the specific rotation of the corresponding eigenstates in the Hilbert space. The K broadest states are pointing into the direction of the K coupling vectors, the other ones are orientated orthogonal to them.

As a result of this local mechanism, the critical value of the coupling strength at which the *last* separation of a broad mode occurs, depends not only on the overall $\bar{\Gamma}/\bar{D}$ but on the local properties of the level density as well. This calls for caution in using $\bar{\Gamma}/\bar{D}$ as a measure for the degree of reorganization of the spectrum. Concerning the total cross section, we found that the interference effects between resonances may lead to an underestimation of resonance widths and transition strengths, especially in the region of critical coupling strength.

Thus, the complete reorganisation of the system is produced by numerous level repulsions of two resonances in the complex plane. It is caused by a mechanism which is efficacious on small energy scales and occurs successively over the full energy range of the spectrum.

The complete figure of hierarchically arranged eigenvalues is produced by local trapping of resonances. The basic process is the repulsion of two complex eigenvalues which we studied analytically and numerically by means of a simple example of two states and one open decay channel.

The few broad modes gain large values of the imaginary part of the complex eigenvalues, or in other words, they get small lifetimes. The number of broad modes is equal to the rank of the external coupling matrix, which is equal to the number of open decay channels. For the rest of the resonances one observes, in spite of the large coupling strength between bound and scattering states, a drift of the eigenvalues backwards to the real axis. The lifetimes of these trapped states are larger by several orders of magnitude than those of the broad modes.

Acknowledgement: This work has been supported by *Deutsche Forschungsgemeinschaft* under the project number *Ro 922/1* and by the *Science and Technology cooperation Germany / Poland* under the project number *X081.39.*

References

[1] P. Kleinwächter and I. Rotter, Phys. Rev. C 32, 1742 (1985)

[2] H. Friedrich and D. Wintgen, Phys. Rev. A 32, 3231 (1985)

[3] V.V. Sokolov and V.G. Zelevinsky, Phys. Lett. B 202, 10 (1988); Nucl. Phys. A 504, 562 (1989)

[4] V.B. Pavlov-Verevkin, Phys. Lett. A 129, 168 (1988); F. Remacle, M. Munster, V.B. Pavlov-Verevkin and M. Desouter-Lecomte, Phys. Lett. A 145, 265 (1990)

[5] F.-M. Dittes, W. Cassing and I. Rotter, Z. Phys. A 337, 243 (1990)

[6] P. von Brentano, Phys. Lett. B 238, 1 (1990); B 246, 320 (1990); Nucl. Phys. A 550, 143 (1992)

[7] I. Rotter, Rep. Prog. Phys. 54, 635 (1991) and references therein

[8] F.-M. Dittes, I. Rotter and T.H. Seligman, Phys. Lett. A 158, 14 (1991)

[9] F.-M. Dittes, H.L. Harney and I. Rotter, Phys. Lett. A 153, 451 (1991)

[10] V.V. Sokolov and V.G. Zelevinsky, Ann. Phys. (N. Y.) 216, 323 (1992) and references therein

[11] F. Haake, F. Izrailev, N. Lehmann, D. Saher and H.J. Sommers, Z. Phys. B 88, 359 (1992)

[12] R.D. Herzberg, P. von Brentano and I. Rotter, Nucl. Phys. A 556, 107 (1993)

[13] W. Iskra, I. Rotter and F.-M. Dittes, Phys. Rev. C 47, 1086 (1993)

[14] A. Mondragon and E. Hernandez, J. Phys. A 26, 5595 (1993); Phys. Lett. B 326, 1 (1994)

[15] K. Someda, H. Nakamura and F.H. Mies, Chem. Phys. 187, 195 (1994)

[16] A. Bürgers and D. Wintgen, J. Phys. B 27, L131 (1994)

[17] W. Iskra, M. Müller and I. Rotter, J. Phys. G 19, 2045 (1993); G 20, 775 (1994)

[18] S.A. Reid and H. Reisler, J. Chem. Phys. 101, 5683 (1994)

[19] U. Peskin, H. Reisler and W.H. Miller, J. Chem. Phys. 101, 9672 (1994)

[20] F. M. Izrailev, D. Saher and V. V. Sokolov, Phys. Rev. E 49, 130 (1994)

[21] W. Iskra, M. Müller and I. Rotter, Phys. Rev. C 51, 1842 (1995)

[22] E. Sobeslavsky, F.-M. Dittes and I. Rotter, J. Phys. A (1995)

[23] V.A. Mandelshtam, H.S. Taylor, C. Jung, H.F. Bowen and D.J. Kouri, to be published

[24] J. J. M. Verbaarschot, H. A. Weidenmüller and M. R. Zirnbauer, Phys. Rep. 129, 367 (1985)

[25] F. Hinterberger, P.D. Eversheim, P. von Rossen, B. Schüller, R. Schönhagen, M. Thenee, R. Görgen, T. Braml and H.J. Hartmann, Nucl. Phys. A299, 397 (1978)

[26] P. Kleinwächter and I. Rotter, J. Phys. G 12, 821 (1986)

[27] A. Geers, J. Kappert, C. Stöck, F. Temps and J.W. Wiebrecht, *Nachrichten der Akademie der Wissenschaften in Göttingen, II. Mathematisch-Physikalische Klasse*, Nr. 2 (1993)

[28] C. Mahaux and H.A. Weidenmüller, *Shell Model Approach to Nuclear Reactions*, Amsterdam: North-Holland, 1969

Fig. 9
The same as Fig. 8 for three values of the coupling strength: $\alpha = 0.08$, $\alpha = 1$ and $\alpha = 4$ (solid curves). The Breit–Wigner–curves calculated from the complex eigenvalues of the two resonances for the same α (dashed curves).

Fig. 1

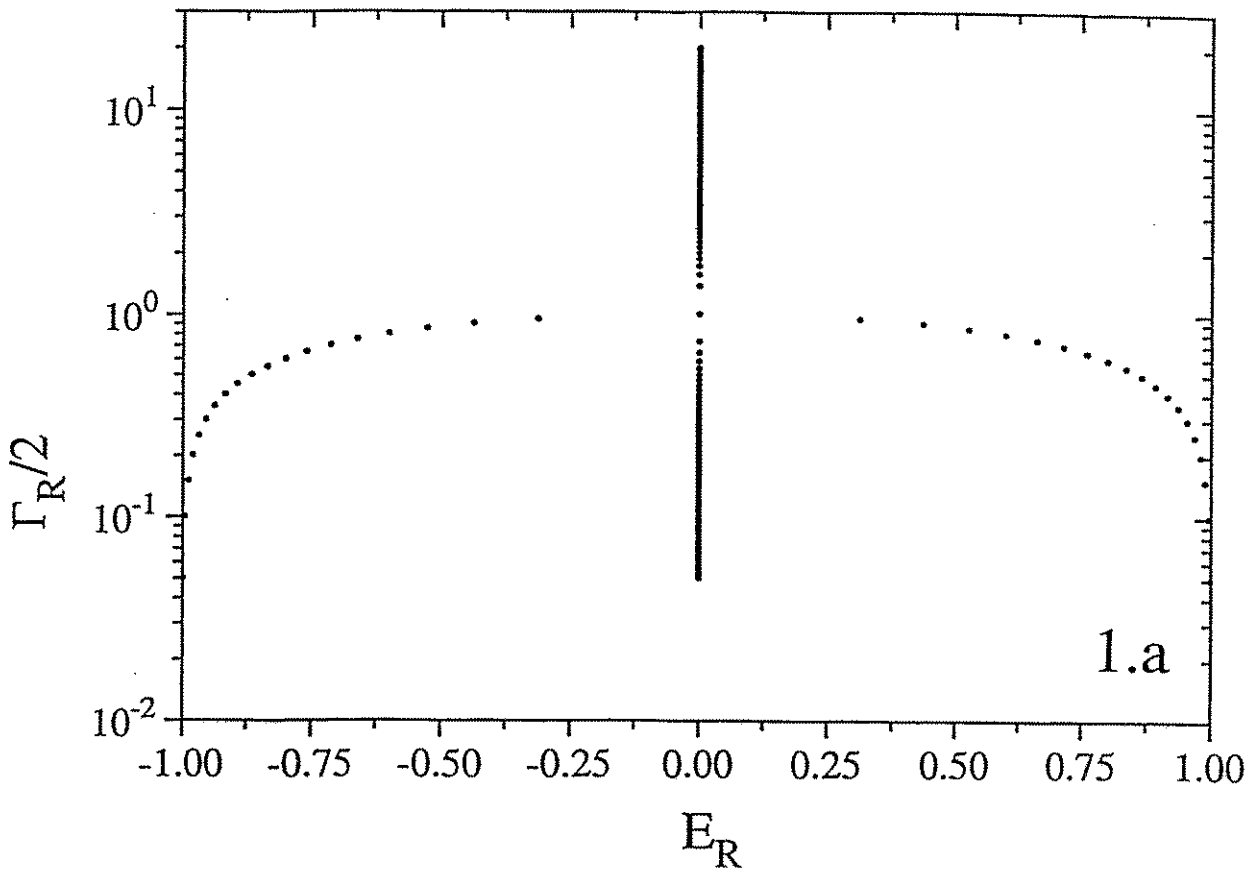
10^1
10^0
10^{-1}
10^{-2}
$\Gamma_R/2$
-1.00
-0.75
-0.50
-0.25
0.00
0.25
0.50
0.75
1.00
E_R
1.a

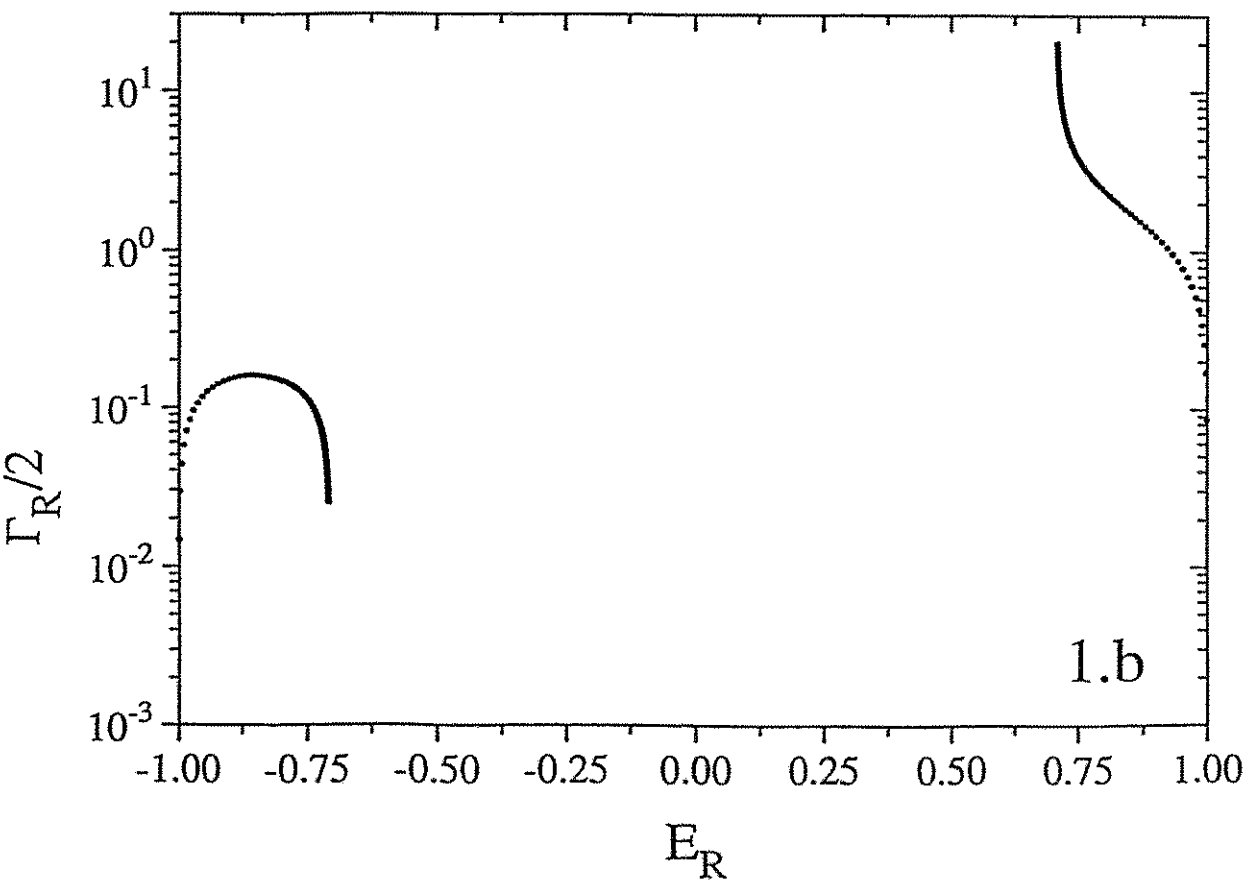
10^1
10^0
10^{-1}
10^{-2}
10^{-3}
$\Gamma_R/2$
-1.00
-0.75
-0.50
-0.25
0.00
0.25
0.50
0.75
1.00
E_R
1.b

Fig. 2

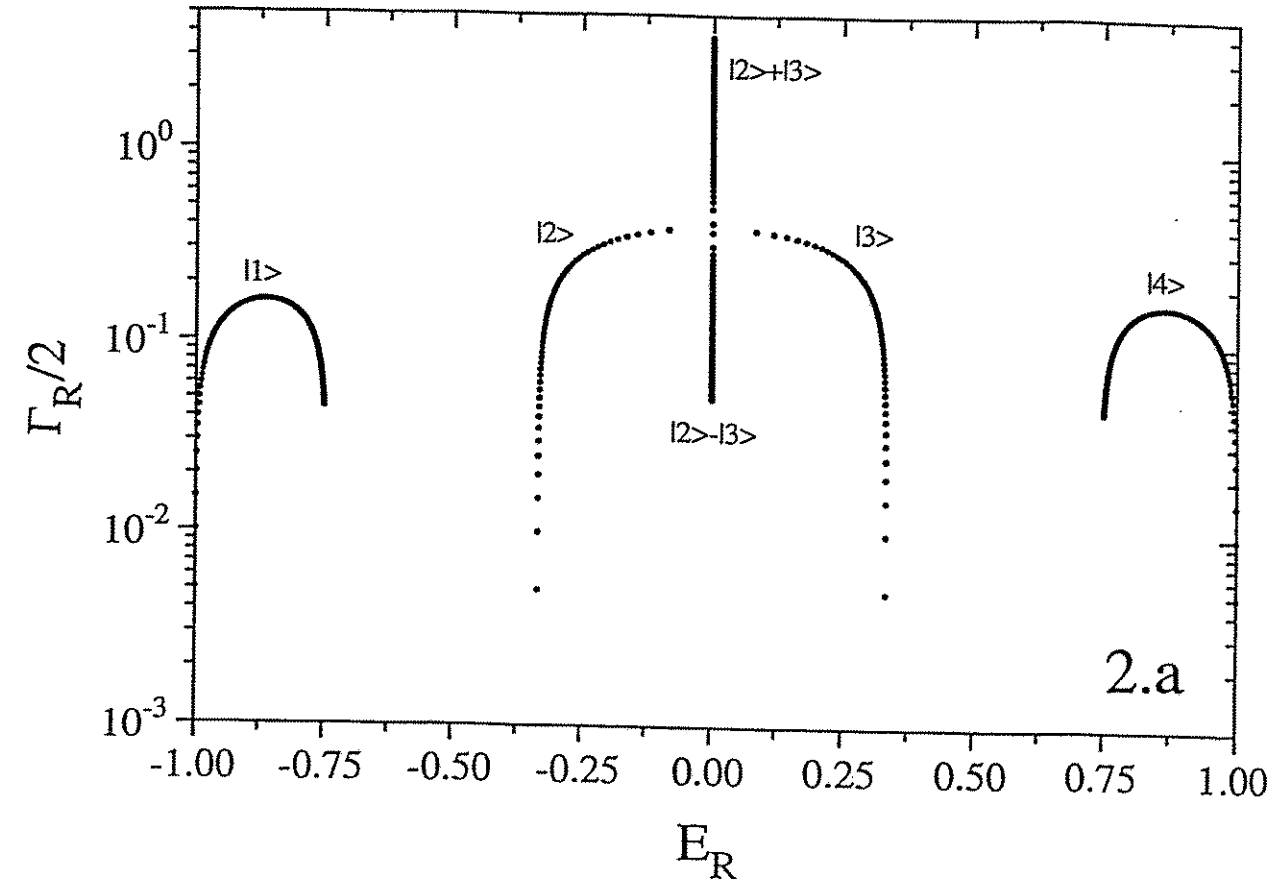
|2>+|3>
|1>
|2>
|3>
|4>
|2>-|3>
10^0
10^{-1}
10^{-2}
10^{-3}
$\Gamma_R/2$
-1.00
-0.75
-0.50
-0.25
0.00
0.25
0.50
0.75
1.00
E_R
2.a

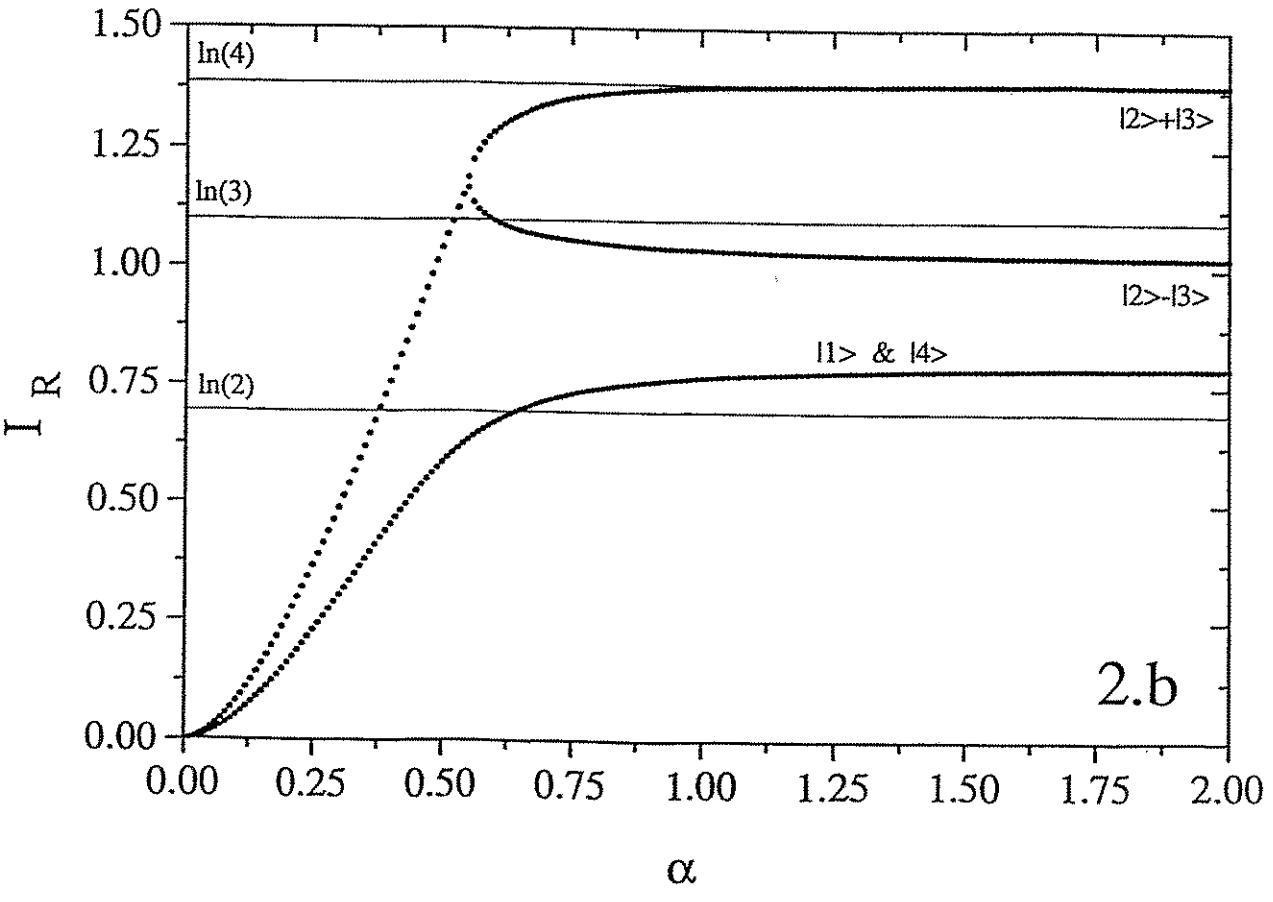
ln(4)
ln(3)
ln(2)
|2>+|3>
|2>-|3>
|1> & |4>
I_R
1.50
1.25
1.00
0.75
0.50
0.25
0.00
0.00
0.25
0.50
0.75
1.00
1.25
1.50
1.75
2.00
α
2.b

Fig. 3

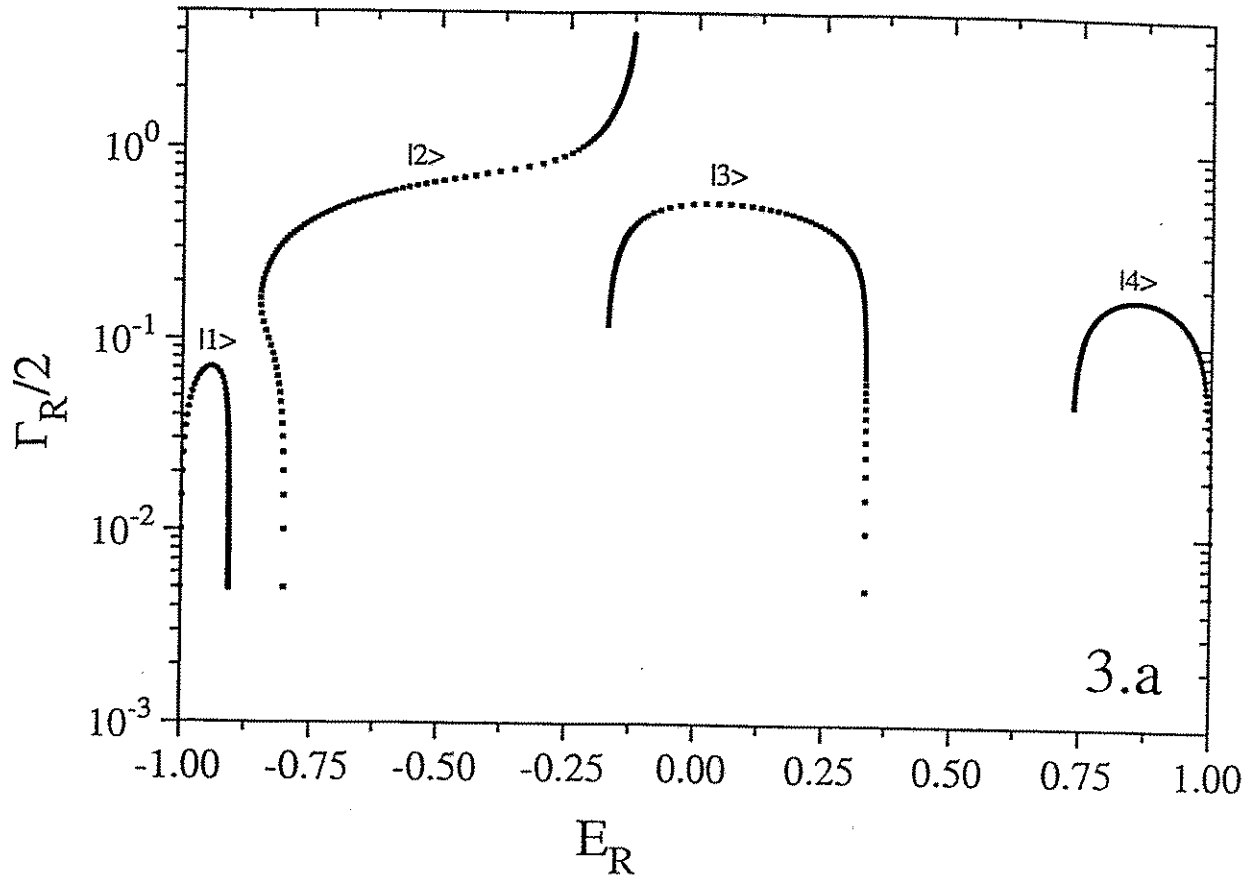
10^0
10^{-1}
10^{-2}
10^{-3}
$\Gamma_R/2$
|1>
|2>
|3>
|4>
3.a
-1.00
-0.75
-0.50
-0.25
0.00
0.25
0.50
0.75
1.00
E_R

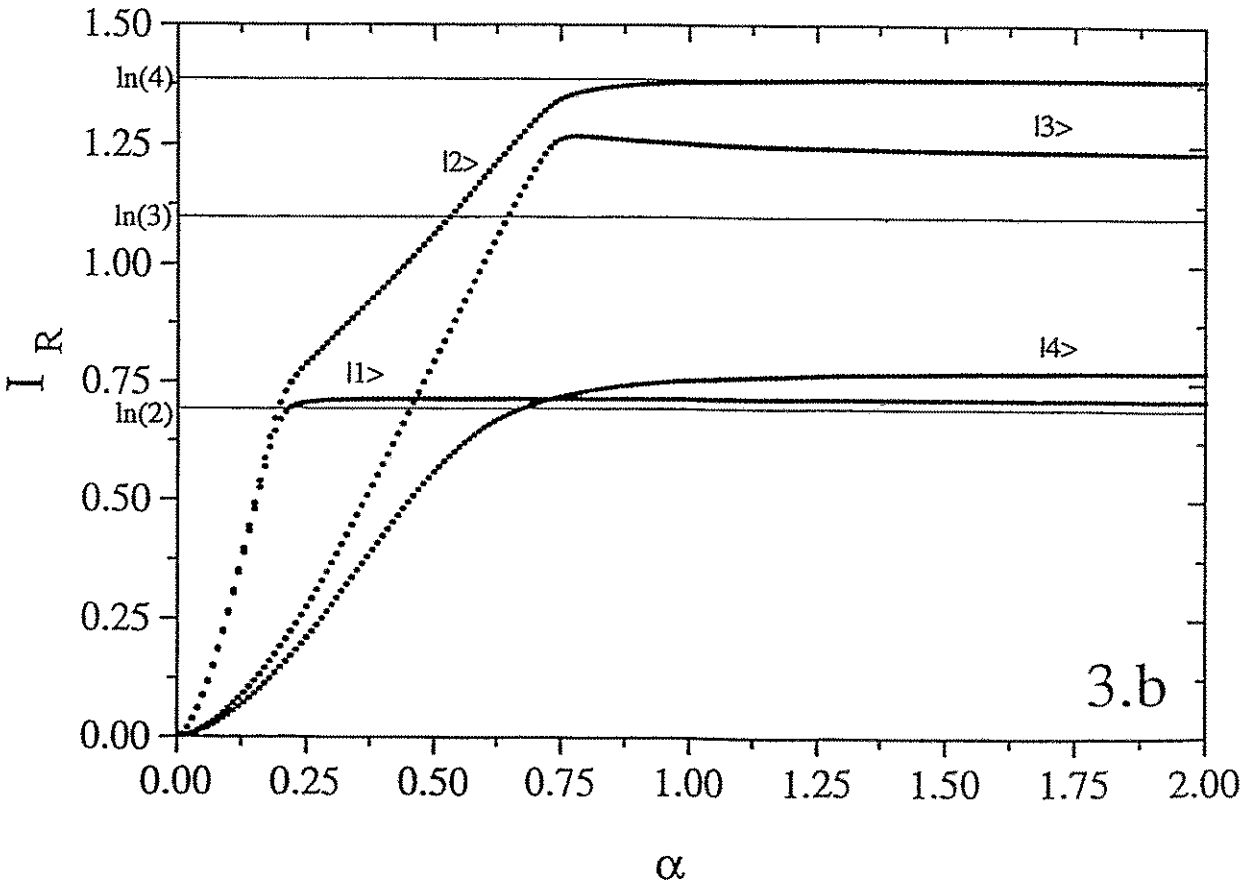
1.50
ln(4)
1.25
ln(3)
1.00
0.75
ln(2)
0.50
0.25
0.00
I_R
|1>
|2>
|3>
|4>
3.b
0.00
0.25
0.50
0.75
1.00
1.25
1.50
1.75
2.00
α

Fig. 4

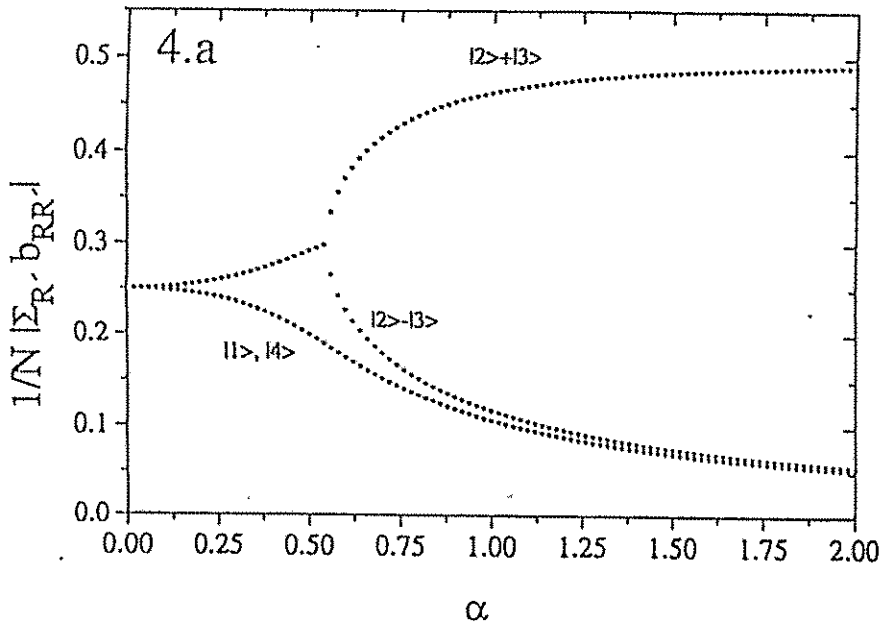
4.a
|2>+|3>
|2>-|3>
|1>, |4>
1/N |Σ_R, b_RR'|
α

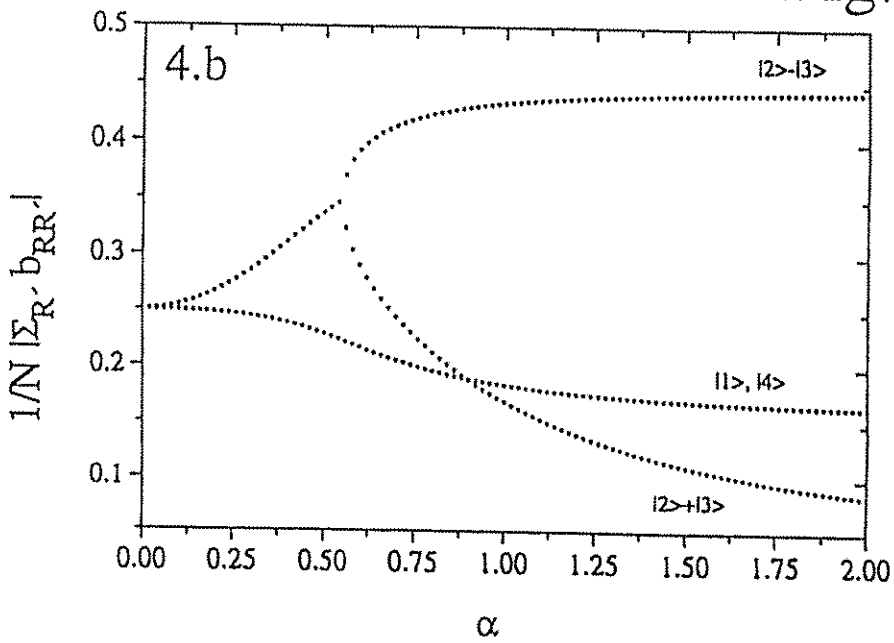
4.b
|2>-|3>
|1>, |4>
|2>+|3>
1/N |Σ_R, b_RR'|
α

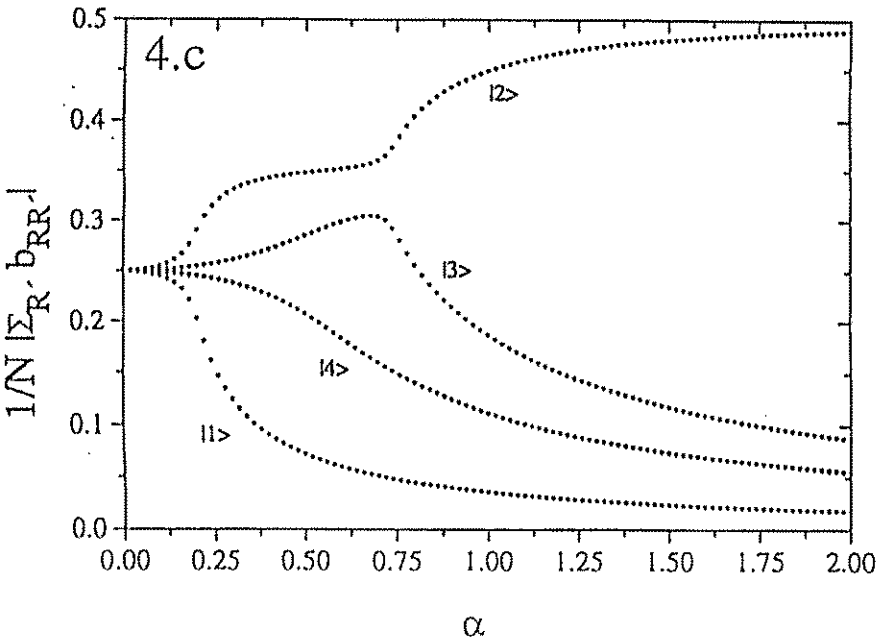
4.c
|2>
|3>
|4>
|1>
1/N |Σ_R, b_RR'|
α

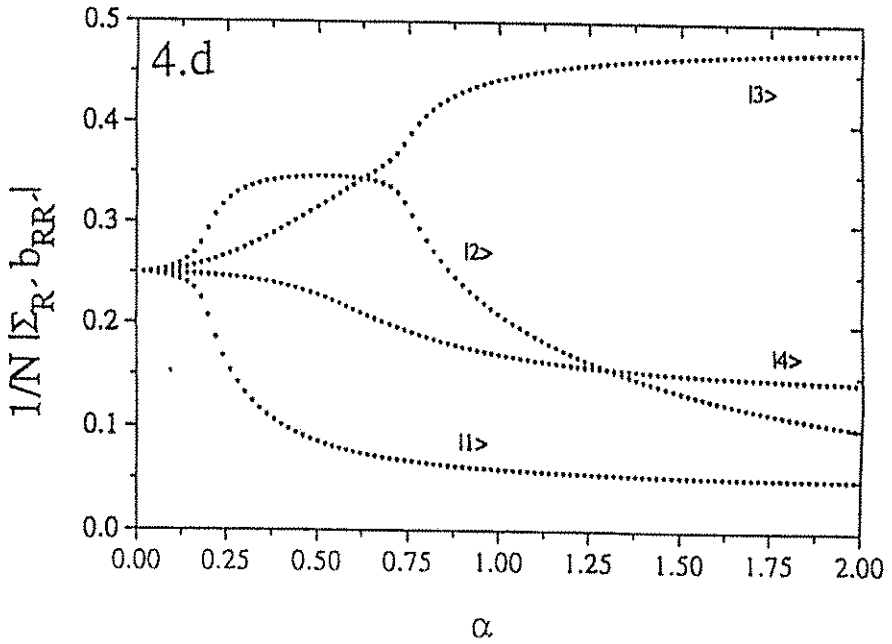
4.d
|3>
|2>
|4>
|1>
1/N |Σ_R, b_RR'|
α

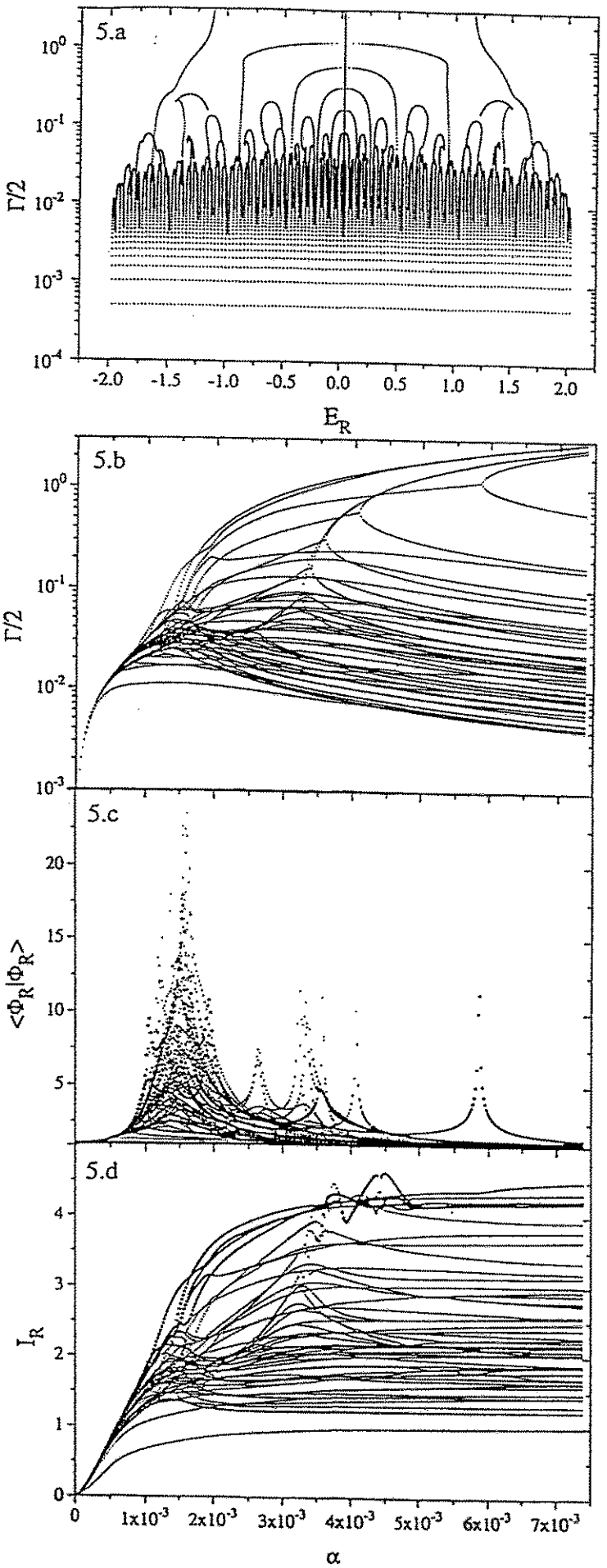
5.a
Γ/2
10^0
10^{-1}
10^{-2}
10^{-3}
10^{-4}
-2.0
-1.5
-1.0
-0.5
0.0
0.5
1.0
1.5
2.0
E_R
5.b
Γ/2
10^0
10^{-1}
10^{-2}
10^{-3}
5.c
$<\Phi_R|\Phi_R>$
20
15
10
5
5.d
I_R
4
3
2
1
0
0
1x10^{-3}
2x10^{-3}
3x10^{-3}
4x10^{-3}
5x10^{-3}
6x10^{-3}
7x10^{-3}
α

Fig. 5

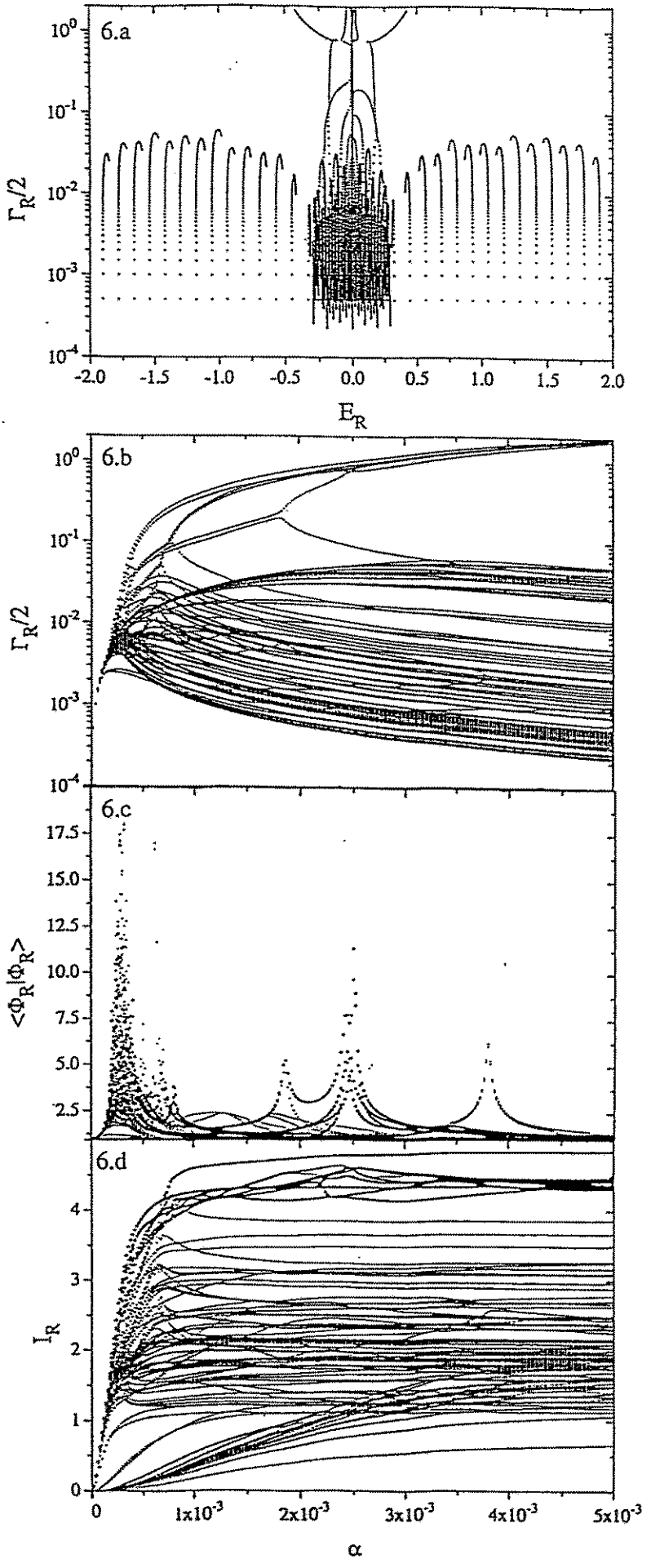
6.a
10^0
10^{-1}
10^{-2}
10^{-3}
10^{-4}
$\Gamma_R/2$
-2.0
-1.5
-1.0
-0.5
0.0
0.5
1.0
1.5
2.0
E_R
6.b
10^0
10^{-1}
10^{-2}
10^{-3}
10^{-4}
$\Gamma_R/2$
6.c
17.5
15.0
12.5
10.0
7.5
5.0
2.5
$\langle\Phi_R|\Phi_R\rangle$
6.d
4
3
2
1
0
I_R
0
1x10^{-3}
2x10^{-3}
3x10^{-3}
4x10^{-3}
5x10^{-3}
α

Fig. 6

Fig. 7

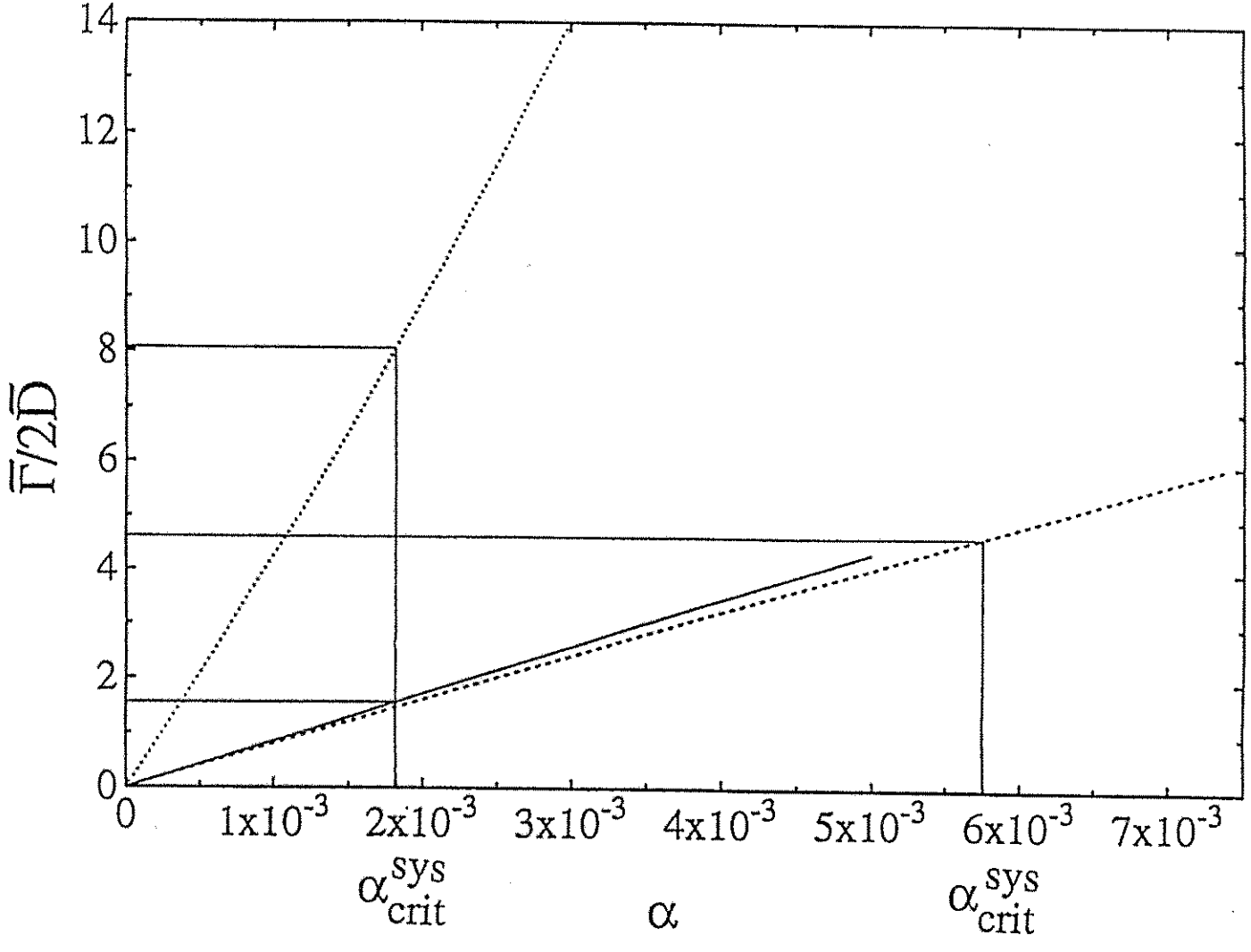
14
12
10
8
6
4
2
0
$\bar{\Gamma}/2\bar{D}$
0
1x10^{-3}
2x10^{-3}
3x10^{-3}
4x10^{-3}
5x10^{-3}
6x10^{-3}
7x10^{-3}
α_{crit}^{sys}
α
α_{crit}^{sys}

Fig. 8

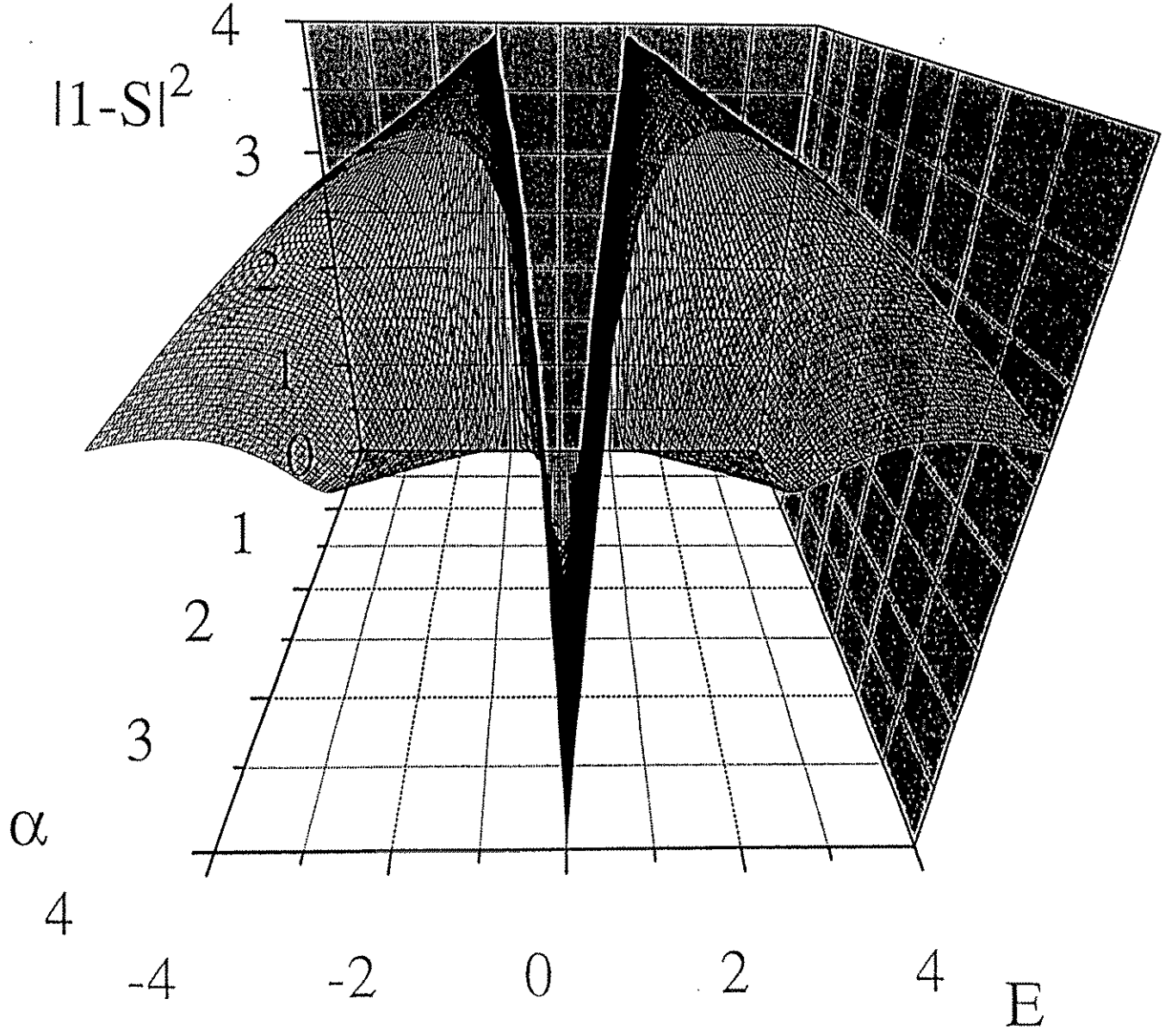

Fig. 9

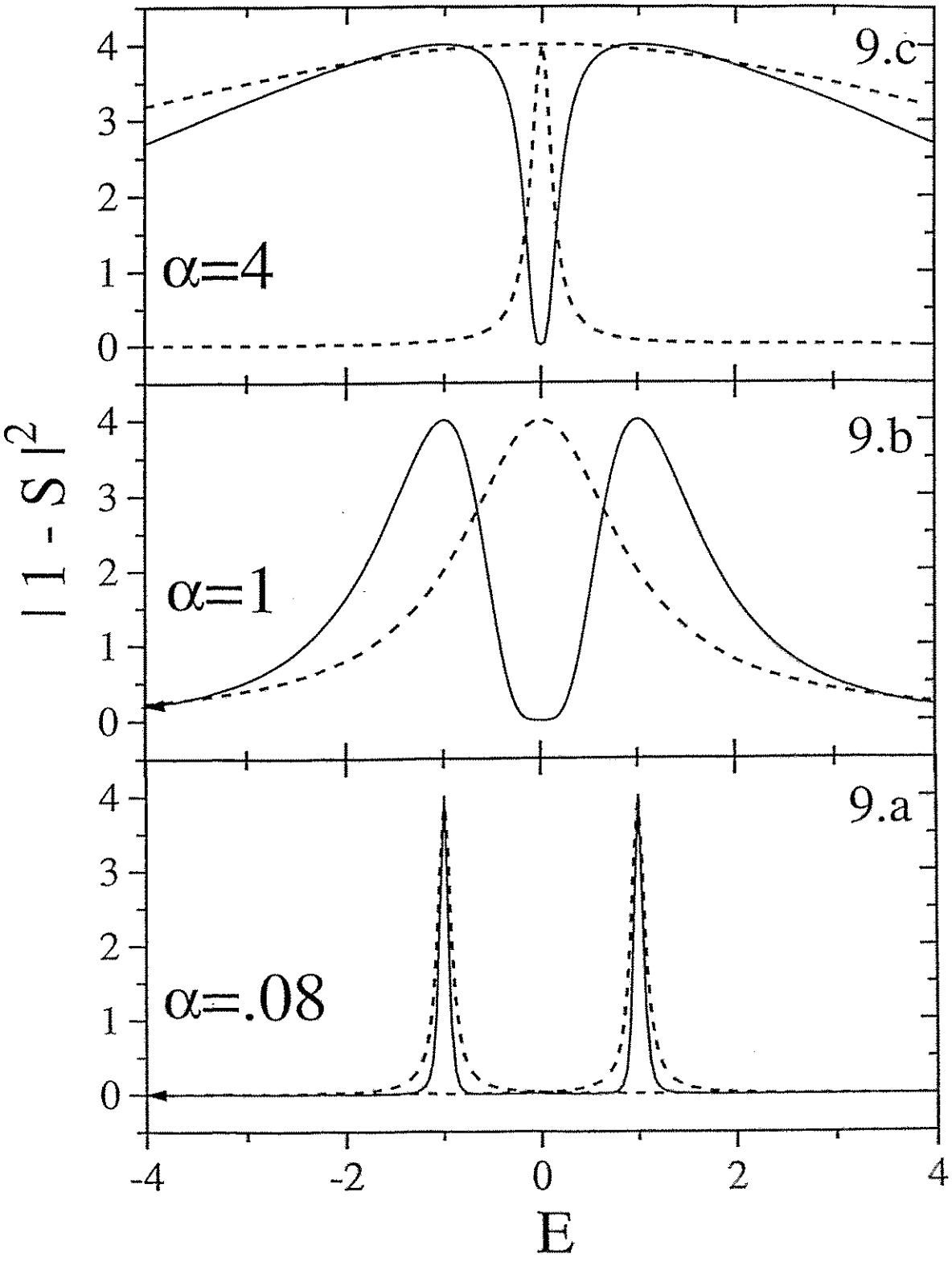

Figure captions

Fig. 1
Propagation of the eigenvalues of H^{eff} in the complex plane with changing α for two resonances and one open decay channel ($N = 2, K = 1$). Fig. (a) corresponds to a symmetrical coupling vector ($\varphi = \pi/4$), Fig. (b) to an asymmetrical one ($\varphi \neq \pi/4$).

Fig. 2
(a): The same as Fig. 1, but for $N = 4$. The eigenvalues of H^0 are chosen symmetrically around $E = 0$. (b): The corresponding mixing functions I_R as a function of α.

Fig. 3
The same as Fig. 2, but for an asymmetric spectrum of H^0.

Fig. 4
Sum of the mixing coefficients $b_{RR'}$ as a function of α for $N = 4$, $K = 1$: (a) and (c) for the completely symmetric coupling vector V_1, (b) and (d) for the asymmetric vector V_2. (a) and (b) correspond to a symmetric spectrum of H^0 (eigenvalues at $E = -1, -1/3, 1/3, 1$), (c) and (d) to an asymmetrical one (eigenvalues at $E = -1, -0.8, 1/3, 1$.

Fig. 5
Propagation of the eigenvalues of H^{eff} in the complex plane with increasing α for the uniform distribution of bound states, $N = 128$, $K = 8$ (a); the resonance widths Γ_R (b), scalar products $\langle \Phi_R | \Phi_R \rangle$ (c), and mixing functions I_R (d) as a function of α.

Fig. 6
The same as Fig. 5, but for the second distribution of bound states described in the text.

Fig. 7
Mean degree of overlap $\bar{\Gamma}/\bar{D}$ as a function of α for bound state distributions 1 (dashed line), 2 (full line) and separately for the region of high level density of distribution 2 (dotted line). The corresponding values of $(\bar{\Gamma}/\bar{D})_{crit}$ and of α_{crit}^{sys} are indicated.

Fig. 8
Total cross section for $N = 2$, $K = 1$ as a function of α.